M. Akgul, Z. Ren, C. T.-C. Nguyen, "Voltage-controlled tuning to optimize MEMS resonator array-composite output power," *Proceedings*, 2011 Joint IEEE Freq. Control Symp. and European Freq. & Time Forum, San Francisco, California, May 1-5, 2011, pp. 753-758.

Voltage-Controlled Tuning to Optimize MEMS Resonator Array-Composite Output Power

Mehmet Akgul, Zeying Ren, Clark T.-C. Nguyen
Department of Electrical Engineering and Computer Sciences
University of California, Berkeley
Berkeley, CA, USA

***Abstract*—A voltage controlled electrical stiffness tuning method has been demonstrated to correct phase and amplitude mismatches between the constituent resonators in a half-wavelength (λ/2) mechanically coupled array-composite towards maximizing its output power. Via tuning, a nine-disk array-composite using 3 output resonators achieves an output current 2.91× larger than that of a single one of its constituent resonators, and only a bit short of the 3× theoretical maximum. Without tuning, the array-composite achieves only 2.78× the current of a single device, and the deviation from ideal is expected to increase with the number of resonators in the array. The amount of tuning available can be tailored in numerous ways, from sizing of electrode-to-disk gap spacing, to specifying the number of devices in the array involved with tuning, to simple variation of voltages across selected electrode-to-resonator gaps. By raising the power output of a high-*Q* micromechanical disk-array composite resonator, the method and design of this work stand to greatly lower the phase noise of oscillators referenced to such devices.**

I. Introduction

Among the various transduction methods [1]-[4] used by micromechanical resonators, capacitive transduction has historically achieved the highest *Q*'s, with values reaching past 160,000 at VHF [3] and 14,600 at 1.2 GHz [4]. Such high *Q*'s, combined with small size and the potential for on-chip integration with CMOS, make this technology very attractive for various applications, from very narrowband low insertion loss filters for RF frequency gating spectrum analyzer implementation [5]; to low phase noise, low power oscillators for radar and communications [6].

Still, adaptation of capacitive micromechanical resonators has so far been slowed by their higher than conventional impedances and limited power handling capability (governed by linearity) relative to other technologies, such as piezoelectric resonators. However, there is no theoretical reason why the impedances and linearities of capacitive resonators cannot achieve the desired levels. In fact, a 60 MHz capacitive resonator recently attained an impedance as low as 140Ω on par with piezoelectric resonators, but with a much higher *Q* >70,000 [7]. The power handling and linearity performance of capacitive transducers has also been studied extensively [8][9], with single 156 MHz capacitively transduced disk resonators demonstrating measured IIP_3's of 19.5dBm that meet GSM requirements.

If even better linearity is needed for more demanding applications, mechanically coupled array-composite resonators, cf. Figure 1, that sum the output currents of identical mechanically coupled resonators designed to resonate in phase, have been shown to improve performance dramatically over stand-alone devices [3][10]. Specifically, arraying reduces motional resistance by increasing the total output current for the same input voltage amplitude; and simultaneously improves linearity by reducing the resonator displacement required to source a given amount of power, thereby reducing the percent of the electrode-to-resonator gap traversed by the mechanical structure. Ideally, arraying improves the linearity and motional resistance by factors equal to the number of resonators used in the array [3]. However, due to fabrication non-idealities, random variations in the resonator and coupling beam dimensions across the array often compromise the degree to which output currents actually add. Because of this, previous array-composites have fallen short of their expected impedance and linearity improvements, especially when the number of resonators used in the array is large [3][10].

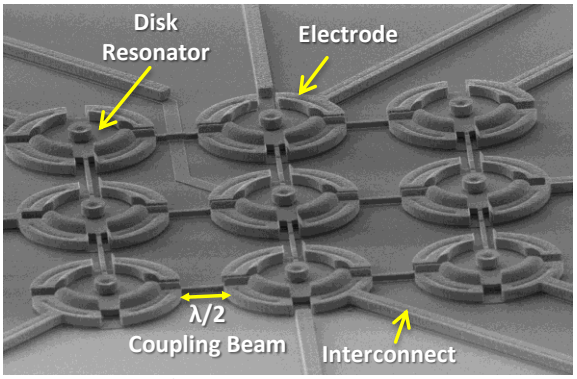

Figure 1: SEM image of a mechanically coupled micromechanical disk array-composite with individual electrode access to each of the resonators constituting the array.

This work attempts to better understand the effect of mismatches between the elements of an array-composite resonator by investigating how stiffness tuning some of the resonators in the array influences the amplitude and phase matching of resonators being summed. In particular, voltage-controlled electrical stiffness tuning applied to several resonators in the array-composite generates maxima in the individual and combined output currents measured off three resonators of the array when 1) their phases are matched; and 2) their phases are close to that of the input drive signal. Tuning over a 7V range induces a measured 16% change in combined array-composite output current, which corresponds to a 1.3dB change in output power that can impact the linearity of a channel-select filter or

The authors would like to thank DARPA for supporting this work.

$$R_x = \frac{f_o\,\gamma\,\rho}{2\,Q\,h\,\varepsilon_o^2}\frac{d_{gap}^4}{V_P^2} \quad (1)$$

f_o : Resonance frequency
h : Resonator thickness
ε_o : Permittivity of vacuum
V_P : DC polarization voltage
γ : Dynamic-to-physical mass ratio
m_{re} : Dynamic mass $m_{re} = \gamma\,\pi\,R_d^2\,h\,\rho$
d_{gap} : Electrode-to-resonator gap spacing
ρ : Density R_d : Disk radius Q : Quality factor

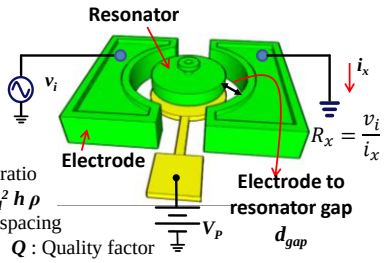

Figure 2: Schematic of a contour mode disk resonator, identifying important design variables and providing the expression for the effective motional resistance R_x of the device.

the phase noise of a high-Q MEMS-based oscillator.

II. High Frequency, High Q, Low Impedance Capacitively Transduced Mechanical Resonators

This work utilizes capacitively transduced radial-contour mode micromechanical disk resonators [11], such as shown in Figure 2. This device consists of a conductive disk suspended by a center stem 700 nm above an electrically contacted ground plane and surrounded by electrodes spaced only 80 nm from the disk edges. A voltage applied to the ground plane, i.e., V_P in the figure, is effectively also applied to the disk itself and creates voltage drops across the disk and each of its electrodes that then activates the capacitive transducer. Under normal operation, a combination of a dc-bias voltage V_P and an ac excitation voltage v_i is applied across one electrode (the input electrode), as shown in the figure. When the frequency of v_i matches the resonance frequency of the disk, the disk begins to vibrate, generating a dc-biased (with V_P) time-varying capacitance at the output electrode that then sources an output current i_o.

Although often maligned for supposedly insufficient electromechanical coupling compared with other transducer choices, e.g., piezoelectric, capacitive transducers are actually among the strongest of the bunch when dimensions scale down to tens of nanometers. To see this, one can employ the expressions for electrode-to-resonator overlap capacitance C_o, motional capacitance C_x, and resonance frequency f_o, for a radial-contour mode disk resonator, given by [11],

$$C_o = \frac{\varepsilon_o A_o}{d_{gap}} \;,\; C_x = \frac{V_P^2}{\omega_o^2\, m_{re}}\frac{\varepsilon_o^2 A_o^2}{d_{gap}^4} \;,\; f_o = \frac{\alpha}{R_d}\sqrt{\frac{E}{\rho}} \qquad (2)$$

where A_o is the electrode-to-resonator overlap area, ω_o is resonance frequency in radians, α is a mode shape dependent constant that equals 0.342 for the fundamental contour mode shape in polysilicon, E is the Young's modulus, and other variables are defined in Figure 2. Combining these yields the equivalent k_t^2 for a capacitively transduced disk resonator:

$$k_t^2 = \frac{\pi^2}{2}\frac{C_x}{C_o} = \frac{1}{4 f_o}\frac{\varepsilon_o}{\gamma\alpha}\frac{1}{\sqrt{E\rho}}\frac{V_P^2}{d_{gap}^3} \qquad (3)$$

From (3), the electrode-to-resonator gap spacing clearly offers a very strong knob by which to tailor electromechanical coupling. Plotting (3) for the case of the 159-MHz disk used in this work versus electrode-to-resonator gap spacing alongside the range for k_t^2 of contour-mode AlN piezoelectric resonators [12][13] yields the curves of Figure 3. The right side of the curve, where electrode-to-resonator gap spacings are large, reveals why capacitive transducers were so maligned: the electromechanical coupling is orders of magnitude lower than that

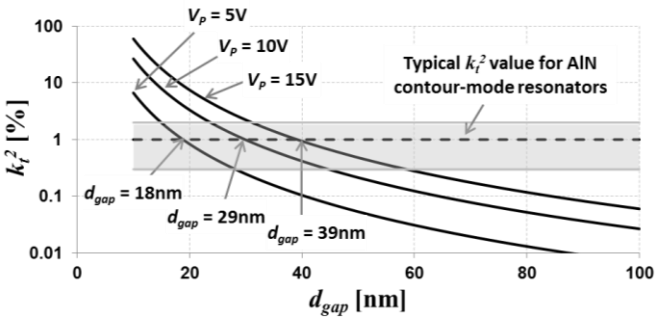

Figure 3: Simulated plot of k_t^2 for a polysilicon contour mode disk resonator operating at 159 MHz, plotted as a function of the electrode-to-resonator gap spacing for three different bias voltages. The shaded band indicates the k_t^2 range for AlN contour-mode resonators in the literature [12][13].

of AlN piezoelectric resonators. However, the left side, where the gap spacing shrinks to tens of nanometers, tells a completely different story. In particular, for the case of V_P =10V, when the gap spacing falls below about 29 nm, a complete reversal occurs, where the electromechanical coupling of the capacitive transducer begins to exceed the typical 1% of AlN contour-mode resonators. The increase in electromechanical coupling with decreasing gap spacing was recently verified in [7], where the electrode-to-resonator gap of a 61-MHz wine-glass disk was reduced to 37 nm from 92 nm to effect a change in motional resistance from 5,350Ω to 140Ω, all while still retaining a Q of 73,173—the only on-chip room temperature resonator in existence able to attain simultaneous high Q >70,000 and low impedance < 150Ω.

Unfortunately, however, the motional resistance of the resonator, as given by the equation in Figure 2, like its coupling coefficient, is inversely proportional to resonance frequency. In other words, the same 37 nm gap that allowed an R_x = 140Ω at 61 MHz in [7] would yield a much higher R_x of 2.3kΩ at 1 GHz. To counteract this increase, more aggressive gap scaling is needed. For instance, to achieve R_x = 50Ω for a polysilicon disk resonator operating at 1 GHz with an assumed Q of 30,000 and a dc bias voltage V_P =10V, the required gap is 9 nm. Needless to say, this is a very small gap that not only begs the question of whether or not such a small gap can be achieved with high yield, but that also raises nonlinearity concerns, since the 3rd-order intermodulation intercept point IIP_3 starts to drop quickly when the gap passes a certain threshold, effectively imposing a "gap scaling limit" [9].

When the gap scaling limit is met, but the impedance requirement still has not been, the next best course of action is to employ one of the other available knobs: either the dc-bias voltage V_P or the disk thickness h. If the supply voltage is limited, then thickness must be increased, which is unfortunate, since this would require a higher aspect ratio, so becomes increasingly difficult as lateral dimensions shrink to attain higher frequencies. Fortunately, the thickness knob is really a knob to change electrode-to-resonator overlap area A_o, which can be increased without increasing thickness by merely using many resonators so that their total combined overlap area increases. This, of course, is the main idea behind the mechanically coupled disk array-composites under study, here.

III. Mechanically Coupled Array-Composite

By summing the output currents of multiple resonators to

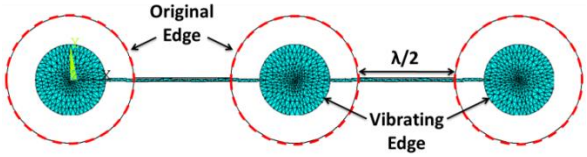

Figure 4: ANSYS modal analysis result for three identical disk resonators mechanically coupled with half-wavelength coupling beams.

attain a larger overlap area and in turn produce a larger total output current, an *N*-resonator array lowers the effective motional resistance linearly with the array size *N*, as described by

$$R_{x,Array} = \frac{v_i}{i_o} = \frac{v_i}{N \times i_x} = \frac{R_x}{N} \qquad (4)$$

where i_x and R_x are the motional current and resistance of a single resonator, respectively; and v_i is input voltage. Note that (4) is valid only when all the resonators generate identical output currents that are in phase and at precisely the same frequency. Given the very high *Q*'s >10,000 of the individual resonators, minute differences between the resonators likely to occur during any practical microfabrication process create slight frequency differences that prevent output currents from adding in phase. As a result, simply connecting the output electrodes of discrete resonators together is not an effective arraying method.

A much better approach uses mechanical coupling beams to physically link the arrayed resonators, as shown in Figure 1. A mechanically linked *N*-resonator array forms an *N* degree-of-freedom system with *N* modal frequencies, each associated with a specific mode shape [10]. This ensures that all resonators resonate at the exact same frequency for a given excited mode, very conveniently eliminating frequency mismatches, allowing same-frequency summing of resonator outputs. Still, most applications, e.g., oscillators, require a frequency response with only one output frequency, not *N* of them. So although its higher power output is welcome, the *N* peaks generated by this mechanically coupled array are not.

One way to eliminate the undesired modes is to use mechanical coupling beams that act as springs with infinite effective stiffness [3]. Specifically, since the coupling beams behave like mechanical transmission lines at this frequency, they can be given infinite effective stiffnesses by merely dimensioning them to correspond to a half-wavelength ($\lambda/2$) at the desired mode frequency. More specifically, the coupling beam lengths should be set equal to an odd multiple of the half-wavelength ($\lambda/2$) of the longitudinal waves travelling in the resonator medium with an acoustic velocity of $\sqrt{E/\rho}$:

$$L_{beam} = \frac{n}{2f_o}\sqrt{\frac{E}{\rho}},\ n = 1,3,5,\ldots \qquad (5)$$

where f_o is the resonance frequency . With effectively infinitely rigid couplers, the mechanically coupled resonators behave as a single array-composite resonator, selectively resonating at a single mode frequency that takes on a shape in which all the resonators move in phase, as shown in Figure 4. The remaining modes are (ideally) pushed to infinity.

In effect, an ideal half-wavelength coupled array of resonators, with its single mode frequency response, effectively realizes an array-composite resonator that behaves like a single of its constituent resonators, except with lower impedance, better linearity, and better power handling capability.

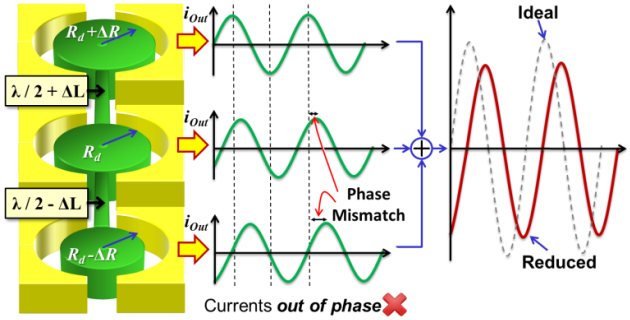

Figure 5: Schematic description of the effect of mismatches between resonators and coupling beams on array performance.

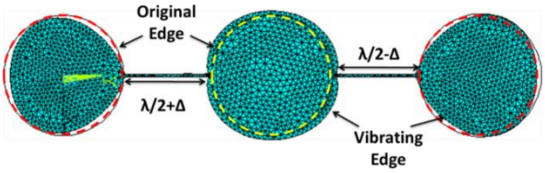

Figure 6: ANSYS simulation for a three-resonator array with 1% error in disk radii and coupling beam lengths in a worst case mismatch scenario.

IV. Effect of Non-Idealities on Arrays

The analysis in the previous section assumes an ideal case, where all the disks that form the array are identical and all coupling beam lengths exactly match the $\lambda/2$ condition of (5) at the common resonance frequency of the disks. In this perfect scenario, all disks resonate in phase and generate identical output currents that lead to the advertised *N*-times reduction in R_x. However, in practice, various process variations in lithography, etching, etc., lead to deviations from a perfect match between the array elements. As a result, the disk radii and coupling beam lengths in the array structure have a random distribution around the ideal design values, as illustrated in Figure 5. Hence, each coupled disk would have a slightly different resonance frequency were it to resonate by itself. Furthermore, variations in the coupling beam lengths create deviations from the half-wavelength condition, meaning the beams are no longer infinitely rigid couplers. Although the mechanical coupling beams still impose a common resonance frequency, they now do so with the following consequences:

1. Different disks reach their resonance displacement maxima at different times. Thus, the output currents generated by individual resonators are not precisely in phase.
2. Mismatches between coupled resonators and coupling beam lengths distort the mode shapes of constituent resonators, causing them to deviate from the ideal circular contour mode shape, as shown in Figure 6, which presents the mode shape predicted by ANSYS for a three-resonator array in a worst case mismatch scenario with 1% error in the disk radii and coupling beam lengths. The result is significant distortion of the mode shape compared to the ideal case of Figure 4. This mode shape distortion diminishes the resonance amplitude of the resonators, which then leads to reduced output current.
3. Spurious modes ensue that are no longer suppressed by infinite stiffness coupling beams.

As a result, even though all the resonators in the array generate an output current precisely at the same frequency—a

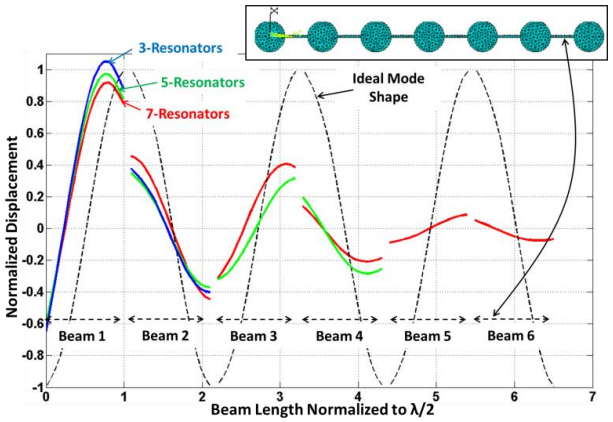

Figure 7: ANSYS harmonic analysis showing coupling beam mode shape displacements (normalized to the ideal mode shape) for mechanically non-ideal coupled disk resonator arrays with varying array sizes (3, 5, and 7 resonators, as marked) for a 1% worst-case dimensional mismatch between the array elements; compared to the ideal mode shape plotted as the dashed curve.

requirement imposed by mechanical coupling—the individual output currents are smaller and out-of-phase, so sum to a value lower than the theoretical maximum, as shown in Figure 5. This underperformance will likely get worse as frequencies rise, since smaller dimensions would likely amplify mismatches, and the larger array sizes needed to maintain low impedance and good linearity would further distort the individual element mode shapes, as verified by the FEA-generated plot of Figure 7. Indeed, any method for tuning out mismatches becomes more important at higher frequencies.

V. Voltage Controlled Electrical Stiffness Tuning of Resonator Array-Composites

Since frequency and stiffness deviations comprise the ultimate consequence of process-induced non-ideality, controlling stiffness is perhaps the best way to counteract such non-idealities. The capacitive transducers used in this work offer a very convenient method for controlling stiffness via mere adjustment of the voltages applied across their capacitive gaps, which changes the electrical stiffness across these gaps. Electrical stiffness [14] arises from the electric field force between the conductive resonator and its parallel-plate electrode that rises and falls as the resonator gets close and far, respectively, from the electrode. This force is in phase with resonator motion, so comprises an effective electrical stiffness k_e, given by

$$k_e = \frac{\varepsilon_o A_o}{d_{gap}^3} V_\Delta^2 \qquad (6)$$

where A_o is the electrode area, and V_Δ is the DC voltage difference between the electrode and the resonator. Note that this electrical stiffness acts to increase the resonator's displacement, so acts to oppose the mechanical stiffness of the resonator. Its effect on the resonance frequency of a single resonator can thus be modeled by

$$f_o = \frac{1}{2\pi}\sqrt{\frac{k_{re}}{m_{re}}} = \frac{1}{2\pi}\sqrt{\frac{k_m - k_e}{m_{re}}} \qquad (7)$$

where k_{re} is the total effective resonator stiffness at the location of the tuning electrode (i.e., usually at its midpoint), obtained by subtracting the electrical stiffness k_e from the mechanical stiffness at that location k_m; and m_{re} denotes the equivalent dynamic mass at that location. Note that for contour mode disks, location is not an issue, but it can be for more

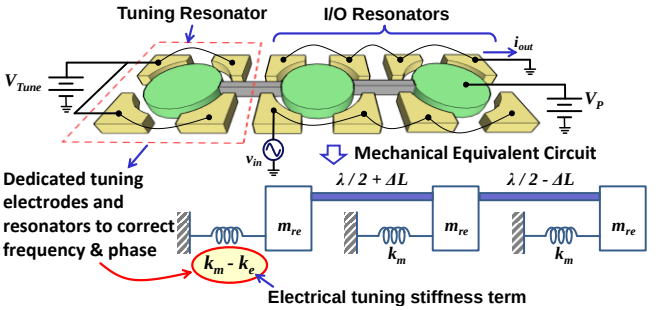

Figure 8: Schematic description of the voltage controlled electrical stiffness tuning method applied to selected tuning electrodes of an array-composite resonator to electrically tune out mechanical mismatches.

general mode shapes, e.g., wine-glass [3][6].

Equation (7) applies very well to individual resonators and has been used successfully to correct the passbands of small percent bandwidth filters, such as in [15], where constituent resonators are coupled by quarter-wavelength beams. For the case of the half-wavelength coupled array resonators of this work, however, (7) must be modified to account for the fact that a half-wavelength coupled array realizes an array-composite resonator with an effective combined stiffness equal to the sum of the stiffnesses of its constituents. Thus, a change in electrical stiffness applied to one resonator, such as shown in Figure 8, affects them all, i.e., affects the whole array-composite. For an *N*-resonator array-composite, where *M* resonators are used for input/output and (*N*-*M*) for frequency tuning, the expression for the array-composite frequency becomes

$$f_o = \frac{1}{2\pi}\sqrt{\frac{Nk_{m,s} - Mk_{e,V_P} - (N-M)k_{e,V_T}}{Nm_{re,s}}} \qquad (8)$$

$$k_{e,V_P} = \frac{\varepsilon_o\, 2\pi R_d\, h}{d_{gap}^3} V_P^2, \quad k_{e,V_T} = \frac{\varepsilon_o\, 2\pi R_d\, h}{d_{gap}^3}(V_{Tune} - V_P)^2 \qquad (9)$$

where $k_{m,s}$ and $m_{re,s}$ are the dynamic stiffness (with no bias voltage) and mass for a single resonator, respectively; while k_{e,V_T} and k_{e,V_P} are the electrical stiffness for a single resonator with and without the tuning voltage V_{Tune} applied to its electrodes, respectively.

Equations (8)-(9) indicate that the amount of tuning available can be tailored in numerous ways, from sizing of electrode-to-disk gap spacing, to specifying the number of devices in the array involved with tuning, to simple variation of voltages across selected electrode-to-resonator gaps. The voltage-control knob provides an especially convenient method to tune individual frequencies so as to minimize mode shape mismatches between the elements of a mechanically coupled resonator array. Note that a designer has a choice of whether to use a constituent resonator in an array composite as an input device, an output device, a frequency tuning device, or any combination of these, including all three.

It should also be noted that the arrays of Figure 1 and Figure 9 do not offer the ability to directly tune the coupling beams. Such tuning is possible with the right design, but most such designs become somewhat cumbersome, so are not implemented here. If coupler tuners are not available, then at least the frequency of the array-composite can be adjusted to minimize the average coupler deviation from half-wavelength at whatever their dimensions. In effect, pulling the resonance

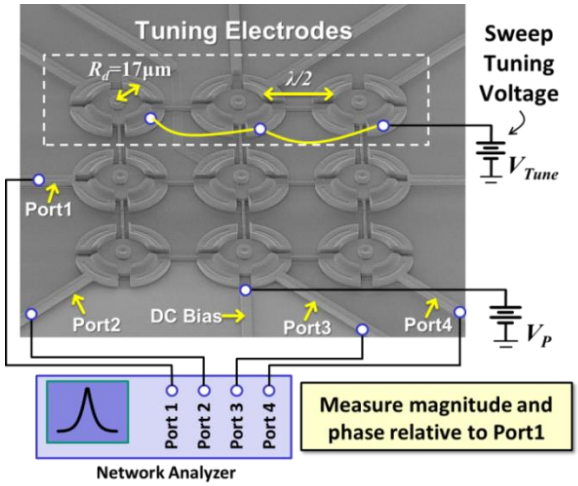

Figure 9: SEM of the fabricated and measured resonator array-composite tuning test structure and schematic of the experimental setup.

frequency closer to the optimum value that provides an average best fit match to the $\lambda/2$ coupling condition for the actual fabricated devices with non-idealities minimizes mode shape distortions and the resulting phase mismatches between individual disk output currents, hence maximizes array output.

VI. Experimental Results

To observe the extent of mismatches stemming from fabrication-induced non-idealities between resonators and the mechanical coupling beams that are otherwise matched in layout, disk array-composites were fabricated in polysilicon using a five-mask fabrication process similar to that of [16]. Figure 9 presents the scanning electron micrograph of a fabricated array structure that differs from previous ones [3] in that (1) it includes electrodes that can individually address each constituent resonator, so provides a mechanism for studying the degree to which an actual fabricated array-composite resonator deviates from the ideal, i.e., the degree to which the phases and resonance amplitudes of its constituent resonators are matched; and (2) it features electrode-resonator combinations specifically equipped to tune the effective electrical stiffness of the entire array structure via adjustment of tuning voltages. The structure consists of nine 17μm-radius contour mode disk resonators designed to operate at 159.8 MHz, with each disk mechanically coupled to its neighbors via half-wavelength beams of length L_{beam} = 26μm to form a 3×3 array-composite resonator.

Figure 9 also includes the test set-up used to gauge the impact of process non-idealities on the disk array-composite and evaluate the efficacy of the proposed corrective tuning method. Here, an Agilent E5071C four-port network analyzer drives the array-composite device into resonance from an input resonator, denoted as Port 1; and simultaneously records the phase and magnitude information of the output currents generated by three output resonators, denoted as Ports 2-3-4. A DC polarization voltage of V_P = 5V is applied common to all disk resonators, and three of the resonators in the array serve as dedicated electrical stiffness tuners, to which a DC tuning voltage separate from V_P is applied to effect selectable amounts of stiffness control. By sweeping the tuning voltage while recording with the network analyzer, the change in the

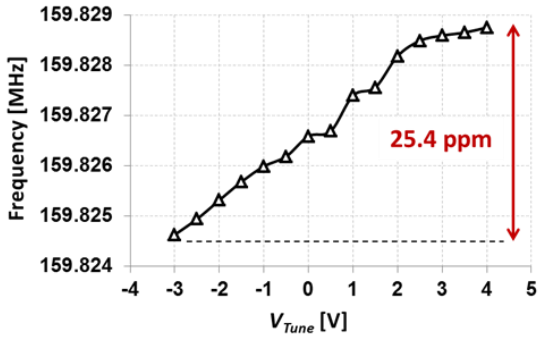

Figure 10: Measured plot of array-composite frequency vs. tuning voltage.

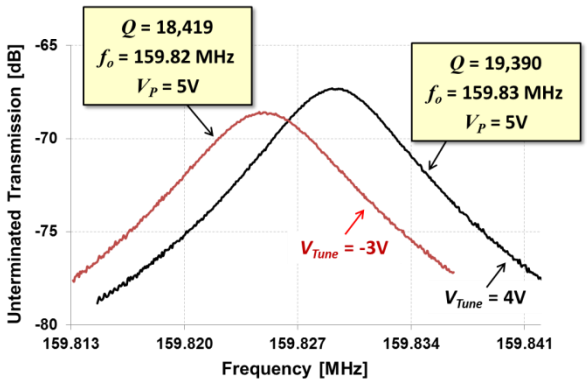

Figure 11: Frequency characteristics for the combined port 2-3-4 output of the array-composite measured at two different tuning voltages.

phase and magnitude of the individual resonators can be plotted as a function of the applied tuning voltage.

To first gauge the amount of tuning provided by the three tuning electrodes, Figure 10 presents a plot of array-composite frequency versus applied tuning voltage. Here, a tuning voltage excursion of 7V provides a 25.4 ppm change in frequency. Although small, this tuning range was still enough to affect noticeable changes in total array output current, as indicated by Figure 11, which plots measured frequency characteristics for the combined output currents from Ports 2-3-4 as a function of the tuning voltage. Here, a 1.3dB change in output is seen over a 7V excursion in tuning voltage.

To better elucidate some of the mechanisms behind tuning-based output improvement, Figure 12 presents measured curves of magnitude and phase of the individual currents generated by each output resonator (ports 2, 3, and 4) plotted as a function of the applied tuning voltage. There are two groups of curves presented in this plot: the solid curves indicate the phase mismatch of each output resonator current relative to the input resonator drive signal, with reference to the *y*-axis on the left; and the dashed curves present the output current amplitudes measured in dBm, with reference to the *y*-axis on the right. The results clearly demonstrate reduction of the phase mismatch between output resonators and input resonator, by more than 20° for the output resonator denoted Port2 as its phase mismatch reduces to almost zero, and by more than 10° for the other two output resonators.

For each output resonator, two maxima are observed: one where the phase of the resonator in question has its lowest phase mismatch with the input resonator; and one where all output resonators are matched in phase. Clearly, phase match-

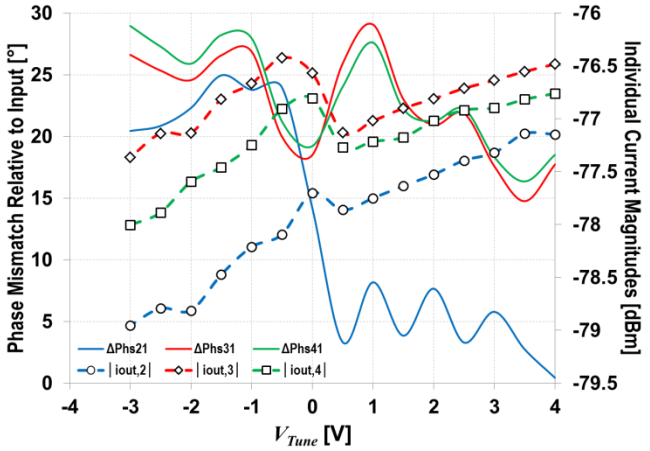

Figure 12: Measured individual output current phase mismatch relative to input (solid line curves – left *y*-axis) and amplitudes (dashed line curves – right *y*-axis) for each output resonator (ports 2, 3, and 4) vs. tuning voltage.

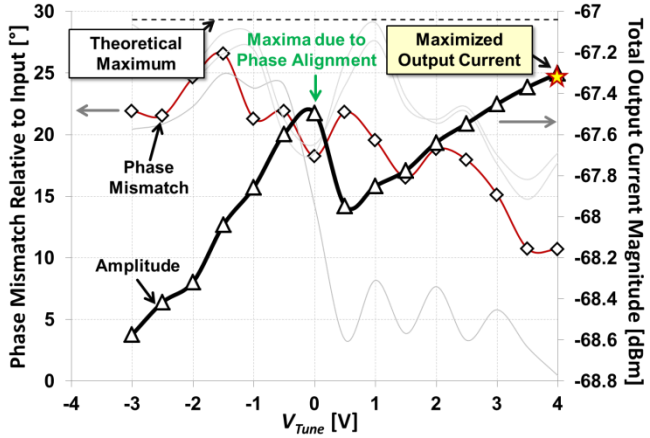

Figure 13: Measured curves of combined total output current phase mismatch relative to input (◇ data markers– left *y*-axis) and amplitude (△ data markers – right *y*-axis), plotted against the applied tuning voltage.

ing is an important consideration for optimized performance of even individual resonators making up an array composite.

Figure 13 plots the phase and amplitude of the total combined output current from the three output resonators against the applied tuning voltage and against a line indicating the maximum output current magnitude expected from an ideal array-composite with no mismatches. Interestingly, for the case of this nine-resonator array-composite, three of which are used for output, the output current is within 2 dB of the ideal over a 7V range of tuning voltage. This might raise questions on the need for tuning at all, but a quick glance at Figure 7 reminds one that a larger array would likely experience a much larger current drop for which correction by tuning would be important. In addition, where transmit power is concerned, every 0.1dB of loss is generally of great concern, especially in space applications. At any rate, Figure 13 attests that voltage-controlled electrical stiffness tuning is clearly an effective means for controlling and minimizing phase mismatches, and more importantly for maximizing the total output current amplitude.

VII. Conclusions

By restoring output power to levels closer to ideal, the described voltage-controlled electrical stiffness tuning method to correct phase and resonance amplitude mismatches between the constituent resonators in mechanically coupled array-composites allows such mechanical circuits to achieve their true potential, even in the midst of finite fabrication tolerances. Clearly, some more refinement in the tuning method, e.g., to allow more precise tuning of individual resonators, would be beneficial, and investigation into just how large an array can be tuned via the described methods is needed. Work towards these continues with the goal of someday making possible assembly of on-chip array-composites employing thousands of capacitively transduced micromechanical resonators to achieve motional resistances down to 1Ω, IIP_3's greater than 50 dBm, and power outputs in the several Watt range, all while retaining the high Q >30,000 typical of such devices.

References

[1] R. C. Ruby, P. Bradley, Y. Oshmyansky, A. Chien, and J. D. Larson III, "Thin film bulk wave acoustic resonators (FBAR) for wireless apps.," in IEEE Ultrasonics Symposium, 2001, vol. 1, p. 813–821.

[2] G. Piazza, "Integrated AlN piezoelectric microelectromechanical system for radio front ends," J. of Vacuum Science & Technology A: Vacuum, Surfaces, and Films, vol. 27, no. 4, p. 776, 2009.

[3] Y. W. Lin, S. S. Li, Z. Ren, and C. T. C. Nguyen, "Low phase noise array-composite micromechanical wine-glass disk oscillator," in Electron Devices Meeting, 2005. IEDM Technical Digest, p. 4–281.

[4] Sheng-Shian Li, Yu-Wei Lin, Yuan Xie,Zeying Ren, C. T.-C. Nguyen, "Micromechanical 'hollow-disk' ring resonators", 17th IEEE Int. Conf. on MEMS, 2004, Tech. Digest, Maastricht, Netherlands, pp. 821-824.

[5] C. T.-C. Nguyen, "Integrated micromechanical RF circuits for software-defined cognitive radio", 26th Symposium on Sensors, Micromachines & App. Sys., Tokyo, Japan, Oct. 15-16, 2009, pp. 1-5.

[6] Y.-W. Lin, S. Lee, S.-S. Li, Y. Xie, Z. Ren, C. T.-C. Nguyen, "Series-resonant VHF micromechanical resonator reference oscillators," IEEE J. Solid-State Circuits, vol. 39, no. 12, pp. 2477-2491, Dec. 2004.

[7] Akgul M., Kim B., "Capacitively transduced micromechanical resonators w/ simultaneous low motional resistance and Q > 70,000", Solid-St. Sens., Actuators and Microsys. Workshop, Hilton Head 2010

[8] R. Navid, J. R. Clark, M. Demirci and C. T. -C. Nguyen, "Third-Order Intermodulation Distortion in Capacitively-Driven CC-Beam Micromechanical Resonators," IEEE MEMS Conf., 2001, Switzerland.

[9] Y. W. Lin, S. S. Li, Z. Ren, C. T. C. Nguyen, "Third-order intermodulation distortion in capacitively driven VHF micromechanical resonators," in IEEE Int. Ultrasonics Sym.,2005, p.18–21.

[10] M. U. Demirci, C. T.-C. Nguyen, "Mechanically Corner-Coupled Square Microresonator Array for Reduced Series Motional Resistance," J. of MEMS, vol. 15, no. 6, pp. 1419-1436, Dec. 2006.

[11] J. R. Clark, W.-T. Hsu, M. A. Abdelmoneum, C. T.-C. Nguyen, "High-Q UHF micromechanical radial-contour mode disk resonators", J. Microelectromech. Syst., vol. 14, no. 6, pp. 1298-1310, Dec. 2005.

[12] G. Piazza, P.J. Stephanou, A.P. Pisano, "One and two port piezoelectric higher order contour-mode MEMS resonators for mechanical signal processing," Solid-State Electronics, vol. 51, 2007, p. 1596–1608.

[13] M. Rinaldi, C. Zuniga, and G. Piazza, "5-10 GHz AlN contour-mode nanoelectromechanical resonators", IEEE 22nd International Conference on MEMS, 2009, p. 916–919.

[14] Harvey C. Nathanson, William E. Newell, Robert A. Wickstrom, and John R. Davis, Jr., "The resonant gate transistor", IEEE Trans. Electron Devices, vol. ED-14, p. 117, 1967.

[15] K. Wang and C. T.-C. Nguyen, "High-order medium frequency micromechanical electronic filters," IEEE/ASME J. Microelectromech. Syst., vol. 8, no. 4, pp. 534-557, Dec. 1999.

[16] J. Wang, Z. Ren, and C. T.-C. Nguyen, "1.156-GHz self-aligned vibrating micromechanical disk resonator," IEEE Trans. Ultrason., Ferroelect., Freq. Contr., vol. 51, no. 12, pp. 1607-1628, Dec. 2004